SIMULATION OF CLUSTER FORMATION IN GAS–SOLID FLOW INDUCED BY PARTICLE–PARTICLE COLLISIONS

E. Wassen and Th.Frank

Research Group on Multiphase Flow, Dept. of Technical Thermodynamics,
Chemnitz University of Technology, 09107 Chemnitz, Germany

Submitted to the International Journal of Multiphase Flow

Abstract–Simulations of gas–solid flows in a horizontal channel are presented. The transient motion of the particle phase is computed using the Simultaneous Particle Tracking technique. Particle–Particle collisions are accounted for by applying a stochastic model. Particle to gas mass loading ratio is varied in the simulations from 0.01 up to 10. The influence of inter–particle collisions on the particle concentration distribution is investigated. Collisions are found to have a significant effect on the concentration distribution at moderate to high loading ratios. For high loading ratios collisions tend to enhance the formation of particle clusters.

Key words: two–phase flow, gas–solid flow, transient simulation, Lagrangian approach, particle–particle collision

1 Introduction

In the industrial fields of energy production and process engineering there are many applications involving gas–particle flows, e.g. pneumatic conveying of granular material, injection of pulverized fuel into burners or separation of solid particles from flue gas. In many cases the particle loading is moderate to high and hence particle–particle interactions significantly influence the flow behaviour. But the average loading is not the only measure for the importance of collisions. Even if the average loading in a particular application is relatively low, there may be regions of locally high concentration, e.g. in "ropes" that form behind pipe bends, where collisions may have a strong macroscopic effect. Additionally there are other factors that may increase the number and importance of collisions. For instance, near obstacles and walls the difference of velocities of impinging and rebounding particles may cause more collisions to occur. These examples indicate that there are many situations in which particle–particle collisions play a significant role and show the importance of taking these collisions into account in a numerical simulation.

In the present paper transient inhomogeneities in particle concentration distribution are examined. These inhomogeneities are induced by inter–particle collisions. Considering the pneumatic conveying of pulverized fuel to a burner the consequence of such a time dependent inhomogeneous concentration distribution is that the burner will not constantly work at maximum efficiency. Furthermore, pressure fluctuations may arise that may cause vibrations or damage. Hence it is important to understand how inhomogeneities develop in time. The present work investigates the influence of particle loading on that effect for gas–solid flows in a horizontal channel.

Considering the Lagrangian type of simulation, i.e. the prediction of macroscopic properties of the dispersed phase by numerically solving the Lagrangian equation of motion of individual particles, various models have been proposed in order to account for inter–particle collisions. The distinct models are closely related to the way the Lagrangian method is applied, which can be done in two principally different ways:

1) *Trajectory Calculation (TC)*: A large number of individual particle trajectories is computed successively. Each trajectory represents a constant flow of particles with identical physical properties. The macroscopic properties of the particulate phase for a certain cell of the numerical mesh are computed by averaging over all trajectory segments that cross that cell. The application of the TC method is limited to the computation of steady flows.

2) *Simultaneous Particle Tracking (SPT)*: In the SPT method the motion of a representative number of particles is calculated simultaneously. Each simulated particle represents a certain number of real particles with identical physical properties. This simulation method is inherently unsteady. The macroscopic properties of the particulate phase for a certain grid cell can be obtained at any time by averaging over all particles that are located in that cell at that time.

In order to take particle–particle collisions into account in the frame of the TC method Oesterlé & Petitjean (1991, 1993) presented an iterative simulation technique. In this technique the collisions were treated stochastically on the basis of macroscopic particle properties obtained from the previous iteration. The technique was used to investigate

a gas–solid flow in a horizontal pipe. The authors showed that collisions significantly influence the vertical concentration profile.

In the frame of the SPT method collisions can be computed either deterministically or stochastically. Tanaka & Tsuji (1991) used a deterministic procedure to simulate a gas–solid flow in a vertical pipe. They found that for higher particle loading the horizontal concentration distribution became more uniform compared to the dilute case. In their deterministic procedure first a collisionless time step was carried out for all particles. After that for each pair of particles it was examined whether these particles had collided during the time step and, if yes, the collision was computed. The computational effort for this procedure is proportional to N^2, let N be the number of simulated particles. For this reason and with respect to the computer resources currently available the deterministic calculation of collisions is of no practical relevancy.

In the great majority of applications of the SPT method collisions are treated stochastically. In that case it is taken advantage of the analogy between the motion of dispersed particles in gas–solid flows and the motion of molecules in dilute gas flows. For simulating the latter the Direct Simulation Monte Carlo (DSMC) method was developed by Bird (1976, 1994). This simulation technique is based on the decoupling of molecular motion and collisions: In every time step first the collisionless motion of all molecules is computed and after that a representative number of collisions is carried out by employing some kind of Monte Carlo method. The DSMC method has been applied to the simulation of gas–particle flows by several authors. Kitron *et al.* (1989, 1990) investigated wall erosion, direct heat transfer and the concentration distribution of impinging streams, respectively. Tanaka *et al.* (1991) and Yonemura *et al.* (1993) examined gas–particle flows in vertical channels. They observed that the flow became unstable and inhomogeneous as the gas velocity decreased and the particle loading increased.

The present paper presents results of transient simulations of gas–particle flows in a horizontal channel. The particle motion was computed using the SPT simulation technique. Particle–particle collisions were accounted for by employing a stochastic model. Special emphasis was put on investigating the effect of particle loading on the formation and development of local regions of higher particle concentration, i.e. "clusters" of particles. A numerical simulation provides the advantage that certain physical effects can be "switched off" and thus effects can be studied seperately that cannot be segregated in an experiment. In real flows with high loading inter–particle collisions as well as phase coupling play an important role. In the present work only the effect of collisions on cluster formation was examined and the influence of phase coupling was not regarded.

The basic equations of fluid motion and their numerical solution are briefly described in section 2. In section 3 the basic equations of particle motion are given. Furthermore, the application of the SPT technique and the stochastic collision model are described in detail. Finally in section 4 results of test case calculations for the horizontal channel are presented and the effect of loading and collisions on cluster formation is discussed.

2 Simulation of fluid motion

The basic equations describing the motion of an incompressible and isothermal gas are the continuity and the momentum equation. In the present work the integral form of these

equations is the starting point for their numerical solution. The integral form is obtained by formulating the mass and momentum balance for an infinitesimal control volume. For the present case the continuity equation reads:

$$\int_S \rho_G \vec{v}_G \cdot \vec{n} \, \mathrm{d}S = 0 \, , \tag{1}$$

where ρ_G is the gas density, $\vec{v}_G$ is the gas velocity, S is the control volume's surface and $\vec{n}$ is the normal vector belonging to the surface element $\mathrm{d}S$. The integral form of the momentum equation reads:

$$\int_S \rho_G \, \vec{v}_G \, \vec{v}_G \cdot \vec{n} \, \mathrm{d}S = \int_S (-p \, \overline{\overline{I}} + \overline{\overline{\tau}}) \cdot \vec{n} \, \mathrm{d}S + \int_\Omega \rho_G \, \vec{g} \, \mathrm{d}\Omega \, , \tag{2}$$

where p is the pressure, $\overline{\overline{I}}$ is the unit tensor, $\overline{\overline{\tau}}$ is the stress tensor, $\vec{g}$ is the gravitational acceleration and Ω is the control volume. As already mentioned in the introduction, in the present work the motion of the gas phase is assumed to be steady and not affected by the presence of particles. Hence equations (1) and (2) neither contain any time dependent terms nor any terms for considering mass or momentum transfer, respectively.

The above equations are solved numerically on the basis of cartesian coordinates. Turbulence is accounted for by using a standard k–ε model. The flow domain is dicretized using block–structured, non–orthogonal, boundary–fitted grids. For discretizing the conservation equations a finite–volume method is used along with a colocated variable arrangement. Pressure–velocity coupling is realized by employing a SIMPLE algorithm.

3 Simulation of the particulate phase

3.1 The motion of a single particle

The motion of every single particle in the gas–particle flow is computed using the Lagrangian approach. The particles are assumed to be solid spheres and the density ratio of particle material and gas is $\rho_P / \rho_G \gg 1$. With that assumption the Lagrangian equation of motion for a single particle of mass m_P reads:

$$m_P \frac{\mathrm{d}\vec{v}_P}{\mathrm{d}t} = \vec{F}_D + \vec{F}_M + \vec{F}_S + \vec{F}_{Gr} \, , \tag{3}$$

where $\vec{v}_P$ is the particle velocity, t is the time and the $\vec{F}_i$ denote the forces acting on the particle. The drag force $\vec{F}_D$ is calculated as:

$$\vec{F}_D = \frac{\pi}{8} \rho_G \, d_P^2 \, c_D \, v_{rel} \, \vec{v}_{rel} \, , \tag{4}$$

with d_P denoting the particle diameter, c_D the drag coefficient, $\vec{v}_{rel}$ the relative velocity between particle and gas and v_{rel} its absolute value. The drag coefficient c_D depends on the particle Reynolds number Re_P:

$$Re_P = \frac{d_P \, v_{rel}}{\nu_G} \, , \tag{5}$$

with ν_G denoting the kinematic viscosity of the gas. In the present work the values for c_D proposed by Morsi and Alexander (1972) were used. The Magnus force $\vec{F}_M$ due to particle rotation is obtained from:

$$\vec{F}_M = \frac{\pi}{8} \rho_G d_P^2 c_M \frac{v_{rel}}{\omega_{rel}} (\vec{\omega}_{rel} \times \vec{v}_{rel}) , \tag{6}$$

where $\vec{\omega}_{rel}$ is the relative rotation between gas and particle:

$$\vec{\omega}_{rel} = \vec{\omega}_G - \vec{\omega}_P , \qquad \omega_{rel} = |\vec{\omega}_{rel}| , \tag{7}$$

with

$$\vec{\omega}_G = \nabla \times \vec{v}_G = \frac{\partial v_G}{\partial x} - \frac{\partial u_G}{\partial y} , \qquad \omega_G = |\vec{\omega}_G| , \tag{8}$$

and the coefficient c_M was chosen according to Tsuji *et al.* (1981). The Saffman force $\vec{F}_S$ due to a shear gradient in gas flow can be calculated from:

$$\vec{F}_S = \frac{1}{4} \rho_G d_P^2 \sqrt{\nu_G} \frac{1}{\sqrt{\omega_G}} c_S (\vec{v}_{rel} \times \vec{\omega}_G) , \qquad c_S = 6.46 , \tag{9}$$

and the gravitational force $\vec{F}_{Gr}$ is:

$$\vec{F}_{Gr} = m_P \vec{g} = \frac{\pi}{6} \rho_P d_P^3 \vec{g} . \tag{10}$$

Other forces like Added–mass force or Basset force can be neglected under the assumption of $\rho_P / \rho_G \gg 1$.

In order to compute $\vec{F}_M$ the particle's rotational velocity $\vec{\omega}_P$ must be known. $\vec{\omega}_P$ can be calculated from:

$$I_P \frac{\mathrm{d}\vec{\omega}_P}{\mathrm{d}t} = \frac{\rho_G}{2} \left(\frac{d_P}{2} \right)^5 c_\omega \omega_{rel} \vec{\omega}_{rel} , \tag{11}$$

where $I_P = 1/10 \, m_P d_P^2$ is the particle's inertia moment and the right hand side of equation (11) denotes the torque exerted on the particle by the fluid as proposed by Dennis *et al.* (1980).

The turbulent velocity fluctuations of the gas phase were accounted for by using the Lagrangian Stochastic–Deterministic (LSD) model by Milojević (1990). In order to simulate wall roughness a model employing an inclined virtual wall as proposed by Sommerfeld (1992) was used.

3.2 The motion of the particle phase

3.2.1 Simulation principle

As already mentioned in the introduction in the present work the formation of particle clusters in gas–particle channel flow was investigated. Such kind of cluster formation was observed by Yonemura *et al.* (1993) who examined upward flows in vertical channels. In their simulations they inserted particles at the bottom of the channels maintaining a constant mass flow. They found that in the upper part of the channels the flow became

inhomogeneous and unstable in space and time as the gas velocity decreased and the particle loading increased. Furthermore, Yonemura *et al.* (1993) showed that the coefficients of restitution e_P and friction f_P for the inter–particle collisions largely affect the growth of clusters.

In contrast to the work of Yonemura *et al.* (1993) in the present work only the effect of particle–particle collisions was examined and the change of gas velocity due to the presence of particles was not accounted for. Of course in reality there is always a strong phase coupling if the particle concentration is as high as in the flows considered here. But the aim of the present work is to contribute to a better understanding of the mechanisms leading to cluster formation. Therefore it is taken advantage of the fact that in a numerical simulation certain physical effects can be examined separately.

The formation and development of particle clusters in space and time is a transient process. For this reason the motion of particles must be calculated time–dependently even if the gas flow is assumed to be steady. The transient particle motion can be computed by applying the SPT simulation technique, i.e. the simultaneous computation of the motion of all simulated particles. The application of the SPT technique along with a stochastic treatment of particle–particle collisions is often referred to as the Direct Simulation Monte Carlo (DSMC) method. The DSMC method was first proposed by Bird (1976, 1994) for the simulation of dilute gas flows. In the present work the following technique was used:

1. A representative number of particles is considered in the simulation, i.e. each simulated particle represents a certain number of real particles.

2. The transient motion of the particle phase is simulated by computing the motion of all particles in successive time steps.

3. The motion of each particle during a single time step Δt is assumed to be decoupled from inter–particle collisions. This assumption is valid if Δt is small compared to mean time between collisions. If a particle collides with a channel wall during Δt the particle–wall collision is carried out according to the rough–wall model mentioned above. After that the calculation of particle motion is continued for the remaining part of the time step.

4. After computing the collisionless motion of a single particle during Δt a stochastic procedure is applied to that particle in order to account for collisions. This procedure is described in the next subsection.

The flow domain is divided into cells which are small compared to spatial changes in the gas flow. The local macroscopic properties of the dispersed phase at a certain time are obtained by averaging over all particles that are located in the same cell at that time.

3.2.2 Treatment of collisions

If the motion of all particles is calculated simultaneously it is theoretically possible to treat the collisions deterministically. Therefore, after every time step one has to examine for every pair of particles in the flow field whether there has been a point of contact during the previous step. If such a point is found the collision between the two particles can be easily

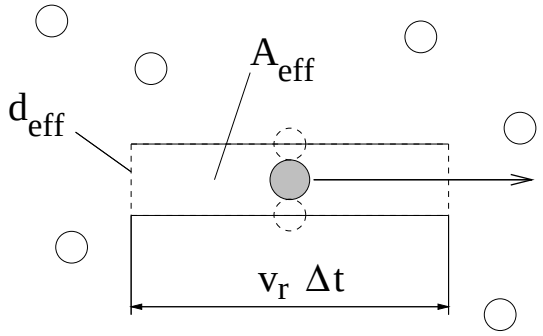

Figure 1: Effective area swept out by a particle moving in a surrounding particle cloud.

computed. This kind of deterministic procedure was used by Tanaka and Tsuji (1991) for simulating gas–particle flows in a vertical pipe. However, this way of treating collisions causes a numerical effort which is proportional to the square of the total number of particles. Even if only the paths of near neighbours, say of all particles in one cell, are compared there is still a proportionality to the total number of molecules in the cell. In order to reduce the numerical effort to a linear proportionality several stochastic procedures have been proposed. In the frame of the DSMC method the Time–Counter method and the No–Time–Counter method were developed by Bird (1976, 1989). The Time–Counter method was also applied to the simulation of gas–solid flows by Kitron *et al.* (1989, 1990). Yonemura *et al.* (1993) used in their simulations the modified Nanbu method proposed by Illner and Neunzert (1987). All these methods are based on randomly selecting a pair of particles that are located in the same cell, computing a collision probability for that selected pair and carrying out the collision according to the acceptance–rejection method. The methods differ in the way of determining how many collisions are actually carried out.

In the present work a stochastic model was used with collisions taking place not between two actually simulated particles but between one simulated and one virtual particle. As decribed above for every time step Δt the motion of all particles in that time step was calculated successively. In order to account for collisions for every particle a stochastic procedure was applied after calculating the collisionless motion of that particle. Considering the two–dimensional case shown in figure 1 the effective area A_{eff} swept out by the particle in the time step Δt, which is small compared to the mean time between collisions τ_c, is:

$$A_{eff} \;=\; d_{eff}\; v_r\; \Delta t \;, \tag{12}$$

where d_{eff} is the effective diameter:

$$d_{eff} \;=\; d_P \;+\; d_{P0} \;, \tag{13}$$

with d_{P0} denoting the mean particle diameter in the surrounding particle cloud, and v_r is the absolute value of the relative velocity between the particle and the surrounding particle cloud:

$$v_r \;=\; |\vec{v}_r| \;=\; |\vec{v}_P \;-\; \vec{v}_{P0}| \;, \tag{14}$$

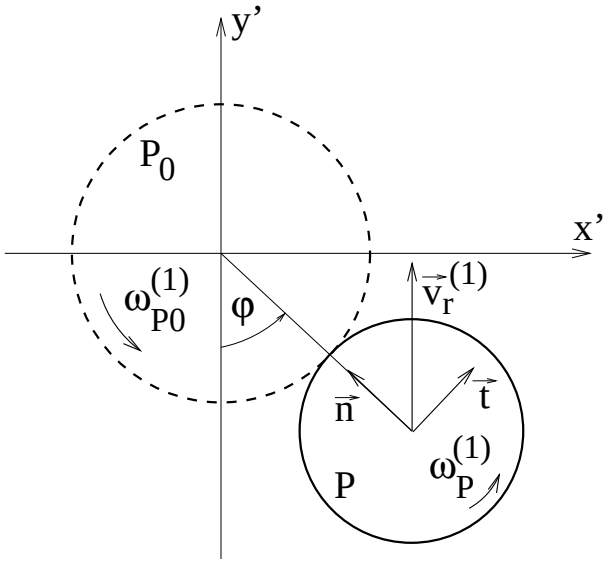

Figure 2: Collision configuration for particle P colliding with virtual particle P_0.

with $\vec{v}_{P0}$ denoting the mean velocity of particles in the cloud. The "surrounding cloud" is assumed to consist of all particles in the cell the particle is located at the end of the time step. Hence d_{P0} and $\vec{v}_{P0}$ are obtained by averaging over all particles in the current cell. The number of particles $N_{A_{eff}}$ that are located in the area A_{eff} and thus the number of collisions with other particles in Δt can be computed from the local number density n_{P0}:

$$N_{A_{eff}} = n_{P0} A_{eff} . \tag{15}$$

Dividing this value by Δt results in the local collision frequency ν_c, i.e. the number of collisions per unit time:

$$\nu_c = n_{P0} (d_P + d_{P0}) |\vec{v}_P - \vec{v}_{P0}| . \tag{16}$$

After computing the collision frequency the collision probability P_c, i.e the probability that the particle undergoes a collision in Δt, is computed as proposed by Oesterlé and Petitjean (1993):

$$P_c = 1 - e^{-\nu_c \Delta t} . \tag{17}$$

The acceptance–rejection method is used to decide whether a collision actually takes place or not. Therefore a random number $\Psi \in [0, 1]$ is generated from a uniform distribution. A collision is decided to take place if $P_c > \Psi$.

As already mentioned above the collision is carried out between the particle currently under consideration and a virtual collision partner. The physical properties of the virtual partner like diameter, velocity and angular velocity are chosen according to the mean values for the current cell. The collision configuration as shown in figure 2 is chosen randomly by generating a collision angle $\varphi \in [-\pi/2, \pi/2]$ from a uniform distribution. The particle's location remains unchanged during the collision and the post–collision velocity

and angular velocity are computed. Since the particle density ρ_P is much larger than the gas density ρ_G the collision duration is much shorter than the particle relaxation time. Hence fluid forces can be neglected during the collision. The post–collision velocities and angular velocities can be calculated by applying the equations of momentum and angular momentum, respectively:

$$\vec{v}_P^{(2)} = \vec{v}_P^{(1)} + \frac{1}{m_P}\,\vec{J}\,, \tag{18}$$

$$\vec{v}_{P0}^{(2)} = \vec{v}_{P0}^{(1)} - \frac{1}{m_{P0}}\,\vec{J}\,, \tag{19}$$

$$\vec{\omega}_P^{(2)} = \vec{\omega}_P^{(1)} + \frac{d_P}{2I_P}\,(\vec{n} \times \vec{J})\,, \tag{20}$$

$$\vec{\omega}_{P0}^{(2)} = \vec{\omega}_{P0}^{(1)} + \frac{d_{P0}}{2I_{P0}}\,(\vec{n} \times \vec{J})\,. \tag{21}$$

Here the subscript $_P$ denotes the particle currently considered, the subscript $_{P0}$ denotes the virtual particle, the superscripts $^{(1)}$ and $^{(2)}$ denote variable values before and after the collision, respectively, $\vec{n}$ is the normal vector of unit length directed from the centre of particle P to the centre of particle P_0 (see figure 2) and $\vec{J}$ is the impulsive force exerted on particle P during the collision. $\vec{J}$ can be decomposed into its normal and tangential components:

$$\vec{J} = J_n\,\vec{n} + J_t\,\vec{t}\,, \tag{22}$$

where $\vec{t}$ is the tangential unit vector pointing in the same direction as the tangential component of the relative velocity between the particles $\vec{v}_r^{(1)}$. By subtracting equation (19) from equation (18), multiplying the resulting equation with $\vec{n}$ and using the relation between the normal components of the pre– and post–collision relative velocities:

$$\vec{v}_r^{(2)} \cdot \vec{n} = -e_P\,(\vec{v}_r^{(1)} \cdot \vec{n})\,, \tag{23}$$

with e_P denoting the coefficient of restitution, the normal component of $\vec{J}$ is obtained by:

$$J_n = -\frac{(1+e_P)\,(\vec{v}_r^{(1)} \cdot \vec{n})}{\dfrac{1}{m_P} + \dfrac{1}{m_{P0}}}\,. \tag{24}$$

Note that J_n is always negative since $(\vec{v}_r^{(1)} \cdot \vec{n})$ is always positive by definition, i.e. the normal component of $\vec{J}$ is always directed towards the centre of particle P. The slip velocity, i.e. the relative velocity between the surfaces of P and P_0, is given by:

$$v_{sl} = \begin{cases} \vec{v}_r^{(1)} \cdot \vec{t} - \omega_P \dfrac{d_P}{2} - \omega_{P0} \dfrac{d_{P0}}{2} & \text{for } \varphi \geq 0\,, \\ \vec{v}_r^{(1)} \cdot \vec{t} + \omega_P \dfrac{d_P}{2} + \omega_{P0} \dfrac{d_{P0}}{2} & \text{for } \varphi < 0\,. \end{cases} \tag{25}$$

v_{sl} is defined as being positive if it is directed in the same direction as the tangential vector $\vec{t}$. Note that $(\vec{v}_r^{(1)} \cdot \vec{t})$ is always positive by definition (see figure 2). In order to

calculate the tangential component of $\vec{J}$ it must be distinguished between the cases of non–sliding and sliding collision, i.e. whether the initial slip between the particle surfaces ceases or not. As shown by Tanaka and Tsuji (1991) and Oesterlé and Petitjean (1993) these cases can be determined by:

1. Sliding collision for $\quad 0 < |J_n| \leq \dfrac{2\,|v_{sl}|}{7\,f_P\left(\dfrac{1}{m_P}+\dfrac{1}{m_{P0}}\right)} \quad : \quad |J_t| = f_P\,|J_n|\,,$

2. Non–sliding collision for $\quad |J_n| > \dfrac{2\,|v_{sl}|}{7\,f_P\left(\dfrac{1}{m_P}+\dfrac{1}{m_{P0}}\right)} \quad : \quad |J_t| = \dfrac{2\,|v_{sl}|}{7\left(\dfrac{1}{m_P}+\dfrac{1}{m_{P0}}\right)}\,,$

where f_P denotes the coefficient of friction. J_t is always directed contrary to the direction of slip velocity and hence is given by:

$$J_t = \begin{cases} -|J_t| & \text{for } v_{sl} \geq 0\,, \\ |J_t| & \text{for } v_{sl} < 0\,, \end{cases} \tag{26}$$

where a positive value of J_t indicates that it points in the same direction as $\vec{t}$. Thus the impulsive force $\vec{J}$ is completely given and by replacing it in equations (18) and (20) the post–collision velocity and angular velocity of the particle P can be computed.

4 Results

4.1 Description of test case

Test case calculations were carried out for gas–particle flows in a horizontal channel. A sketch of the channel geometry is given in figure 3. As shown in this figure the flow is simulated only in a segment of the channel and periodic boundary conditions are used at the left and right boundary of the geometry. Any particle that crosses one of these boundaries is inserted again at the opposite boundary by retaining all of its current physical properties.

The gas velocity and turbulence properties were assumed to be those of a developed turbulent channel flow and to be constant over channel length. These properties were obtained in a preliminary calculation. As mentioned above, despite the relatively high particle loading considered in this work the gas flow properties remained unchanged in the simulations in order to investigate solely the effect of inter–particle collisions.

The physical and numerical parameters used in the present simulations are summarized in table 1. Most of the physical parameters were chosen according to Oesterlé and Petitjean (1993) who carried out simulations for horizotal pipe flows. In the present work flows with different mass loading ratios η were computed. For $\eta = 0.01$ the flow was assumed to be dilute and particle–particle collisions were not considered. For all other loading ratios collisions were simulated according to the stochastic procedure described above. The particles' initial locations were distributed randomly across the flow domain to achieve a uniform initial concentration distribution. The initial axial velocity was chosen

as 0 m/s and the transverse velocity was obtained as a random number from a Gaussian distribution with a mean value of 0 m/s and a standard deviation of 1 m/s.

The use of periodic boundary conditions implicates that the total number of simulated particles in the flow domain $N_{P,tot}$ remains constant throughout the computation. Also the mean particle number density n_{P0}, i.e. the mean number of particles per unit volume, remains constant whereas the local number density n_P changes. The particles are redistributed in the course of a simulation due to fluid forces, gravity, particle–wall collisions and particle–particle collisions.

4.2 Results of simulations

In figure 4 the vertical distribution of the relative number density n_P/n_{P0} is shown for different mass loading ratios. The results of the present work are compared to those obtained by Oesterlé and Petitjean (1993) for a horizontal pipe flow by applying the Trajectory Calculation technique. The data of Oesterlé and Petitjean (1993) were taken at a distance of $L = 6m$ from the inlet cross section of the pipe. In preliminary simulations it had been found that the average time particles need to move that distance under the given conditions is $t = 0.3\,s$. Accordingly in the present work this period of time was chosen as the total physical time to elapse in one simulation run. The two–dimensional distribution of relative number density at $t = 0.3s$ was averaged in axial direction for different distances from the channel bottom and the resulting vertical concentration distribution is shown in figure 4.

For the dilute case ($\eta = 0.01$) the particle concentration is almost uniformly distributed over channel height. The particles in the flow are strongly resuspended due to collisions with the rough walls at the channel top and bottom. For the pipe flow the number density in the lower part of the pipe is higher than in the upper part. In contrast to the two–dimensional simulations of the present work in a three–dimensional pipe a particle colliding with a wall has one more degree of freedom concerning the post–collision translational velocity. For this reason the vertical component of the post–collision velocity is generally smaller in a pipe than it is in a channel. Hence rebounding particles in a pipe flow reach only a smaller height and the particle concentration in the lower region is higher.

With increasing particle loading the concentration profile becomes more non–uniform. The concentration in the upper part decreases and in turn it increases in the lower part. This effect is caused by particle–particle collisions. Particles moving upwards after bouncing against the bottom wall collide with other particles in the inner region of the flow field. As a consequence the maximum height these rebounding particles are able to reach is smaller than in the collisionless case and thus particles tend to concentrate in the lower part of the flow domain. Under certain conditions the maximum number density is observed not closest to the channel bottom but at a certain distance from that wall (see results for channel flow for $\eta = 5, \eta = 10$, and for pipe flow for $\eta = 2, \eta = 10$). In these cases a kind of "shielding" effect occurs. Rebounding particles that move upwards meet particles moving downwards due to gravity. A zone develops where a large number of inter–particle collisions take place. Due to the collisions the vertical velocity component of upward moving particles is reduced and likewise the vertical velocity component of

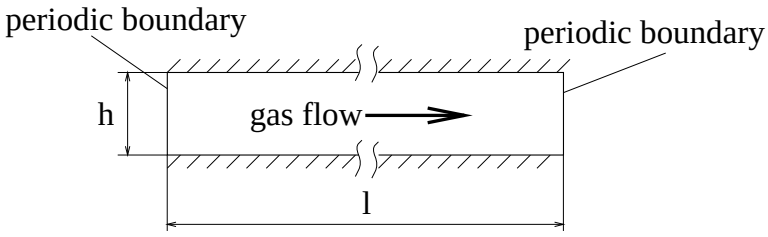

Figure 3: Geometry of horizontal channel for simulation.

Property	Symbol	Value
Channel height	h	0.03 m
Channel length	l	0.8 m
Gas density	ρ_G	1.21 kg/m^3
Kinematic viscosity of gas	ν_G	$1.48 \cdot 10^{-5}$ m^2/s
Gas bulk velocity	U_G	25.5 m/s
Mean particle diameter	$\overline{d}_P$	100 μm
Particle material density	ρ_P	2620 kg/m^3
Coefficient of restitution for particle–wall collision	e_W	0.9
Coefficient of friction for particle–wall collision	f_W	0.53
Coefficient of restitution for particle–particle collision	e_P	0.95
Coefficient of friction for particle–particle collision	f_P	0.4
Mass loading ratio	η	0.01, 1, 2, 5, 10
Number of grid cells	–	128×16
Total number of simulated particles	$N_{P,tot}$	10 000
Time step	Δt	$2 \cdot 10^{-5}$ s

Table 1: Physical and numerical simulation parameters.

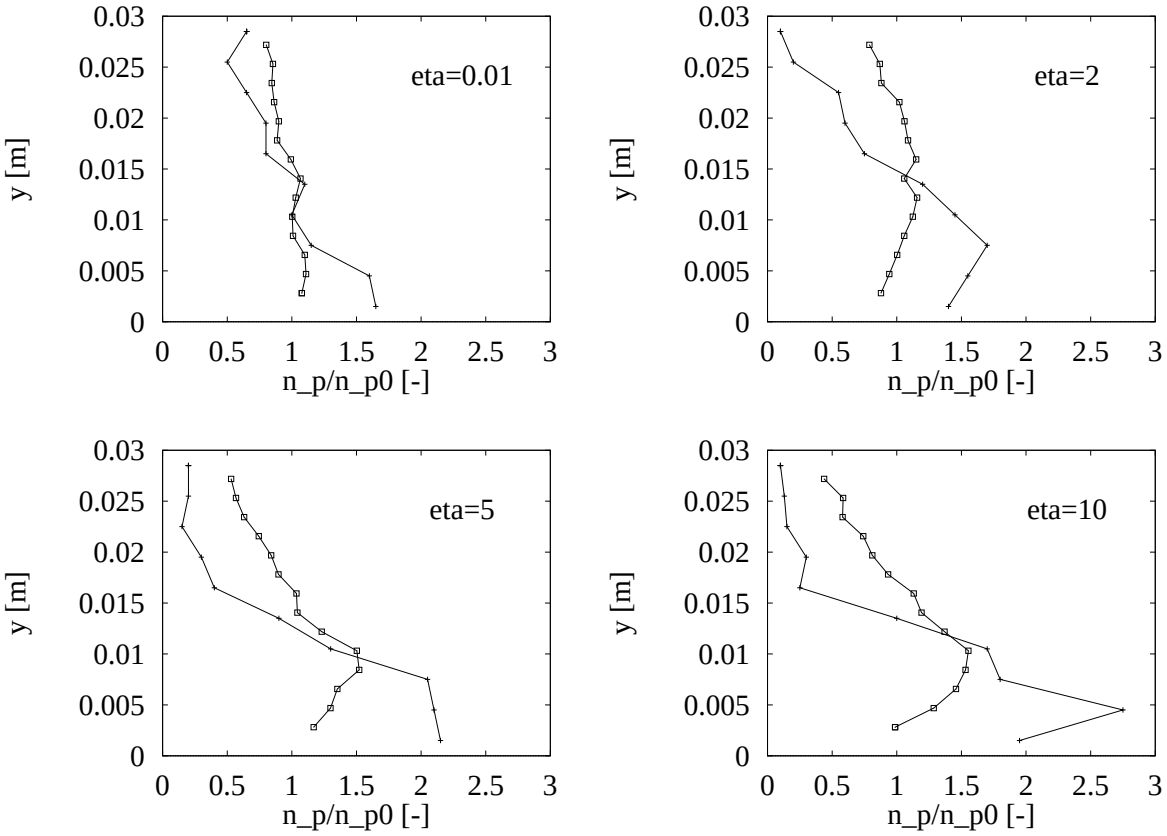

Figure 4: Vertical distribution of relative number density; □ this work ($t = 0.3\ s$), + trajectory calculation Oesterlé and Petitjean (1993) for horizontal pipe ($L = 6\ m$).

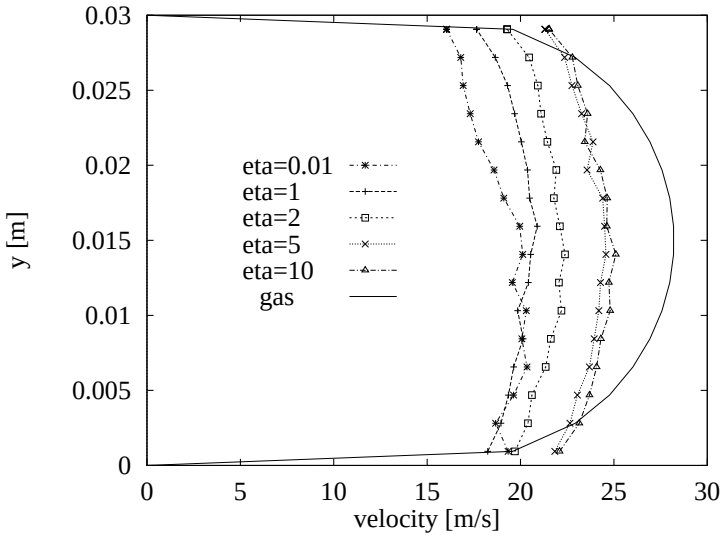

Figure 5: Vertical distribution of mean axial velocity.

downward moving particles. As a consequence a region of higher particle concentration develops and the bottom wall is protected from impacting particles. A similar kind of shielding effect was reported by Kitron *et al.* (1989).

In figure 5 the profile of the mean axial velocity is shown for different loading ratios and for comparison also the gas velocity profile is shown. Like the concentration profile discussed above also the velocity profile was obtained at $t = 0.3\,s$ by averaging the local velocity in axial direction. In the dilute case the maximum axial velocity is observed below the channel axis whereas in all other cases the maximum velocity is found close to the axis. In all cases the velocity decreases towards the channel walls. This is due to the particle–wall collisions, which because of friction and inelasticity reduce the particles' kinetic energy. Hence after a wall collision a particle's absolute velocity is lower than before and the particle is accelerated again by the gas flow as it moves back from the wall into the flow field. In figure 5 it can also be seen that the particles' mean axial velocity increases as the loading increases. With increasing loading the particles undergo more and more inter–particle collisions. These collisions cause the vertical component of particle motion to be damped. As a result the number of collisions with the channel walls decreases. In other words, the mean time between two wall collisions increases. Hence the particles spend more time in the inner region of the flow field und can be accelerated by the gas up to a higher velocity.

The development of particle concentration distribution in space and time for the different loading ratios is shown in figures 6–10. In each of these figures the distribution of relative number density n_P/n_{P0} in the channel is given at seven different times. Note that for the reason of a more convenient representation the channel geometry is shown compressed in horizontal direction. As mentioned above, all simulations start with a randomly generated particle distribution, i.e. at $t = 0\,s$ is $n_P/n_{P0} \approx 1$ all across the channel. After starting the simulation the particles are accelerated in horizontal direction by fluid forces and in downward direction by gravity. The latter is the reason for the increase of number density in the lower half of the channel, which can be observed for all loading ratios at $t = 0.05\,s$. For the dilute case ($\eta = 0.01$), which is shown in figure 6, this inhomogeneity in the vertical concentration distribution can still be found at $t = 0.1\,s$. As the simulation for $\eta = 0.01$ progresses further the concentration becomes almost uniform again, because the particles are redispersed due to irregular bouncing with the channel walls.

In contrast to the dilute case for the cases of $\eta = 1$ and $\eta = 2$ the inhomogeneity in vertical concentration distribution is not observed anymore at $t = 0.1s$ (see figures 7 and 8, respectively). Obviously for these loading ratios particles are redispersed quicker. This is a result of the momentum exchange induced by particle–particle collisions. Particles that have bounced against the bottom wall in an early stage of the simulation move upwards and collide with particles that still move downwards. Thus particles are redistributed evenly. For $\eta = 1$ the concentration distribution remains almost uniform throughout the rest of the simulation. For $\eta = 2$ the development of a region of higher concentration can be observed. The center of this region is located close to the channel axis and the maximum number density in this region is about three times higher than the mean number density.

For the loading ratios of $\eta = 5$ (see figure 9) and $\eta = 10$ (see figure 10) the inhomogeneity of concentration distribution in vertical direction at $t = 0.05\,s$ appears more distinct than

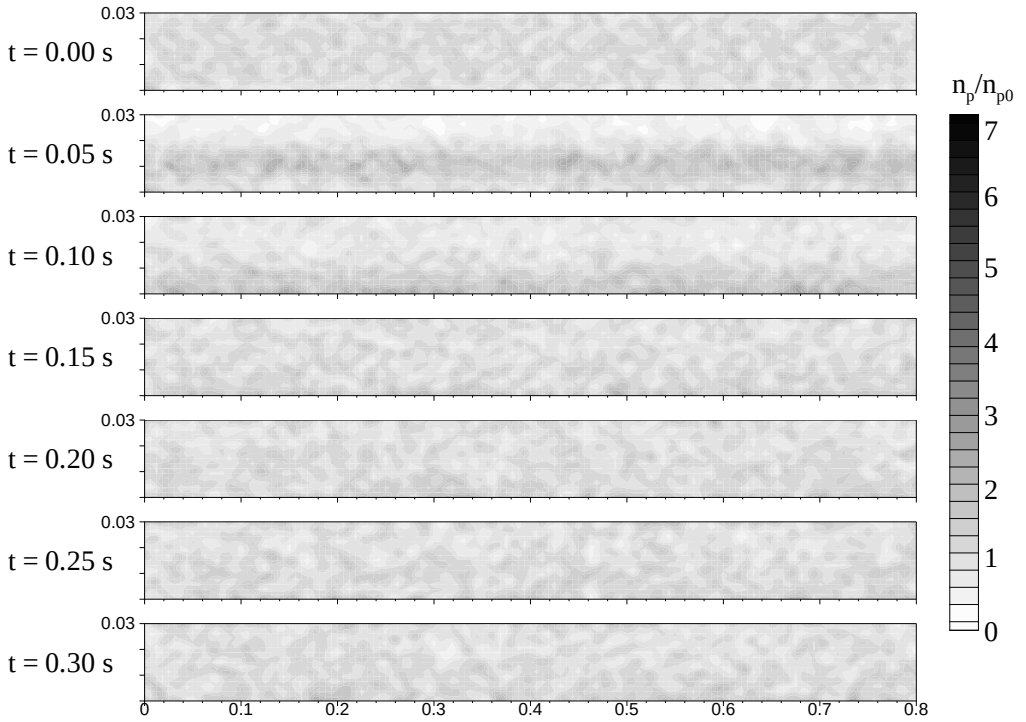

Figure 6: Distribution of relative number density over time for $\eta = 0.01$.

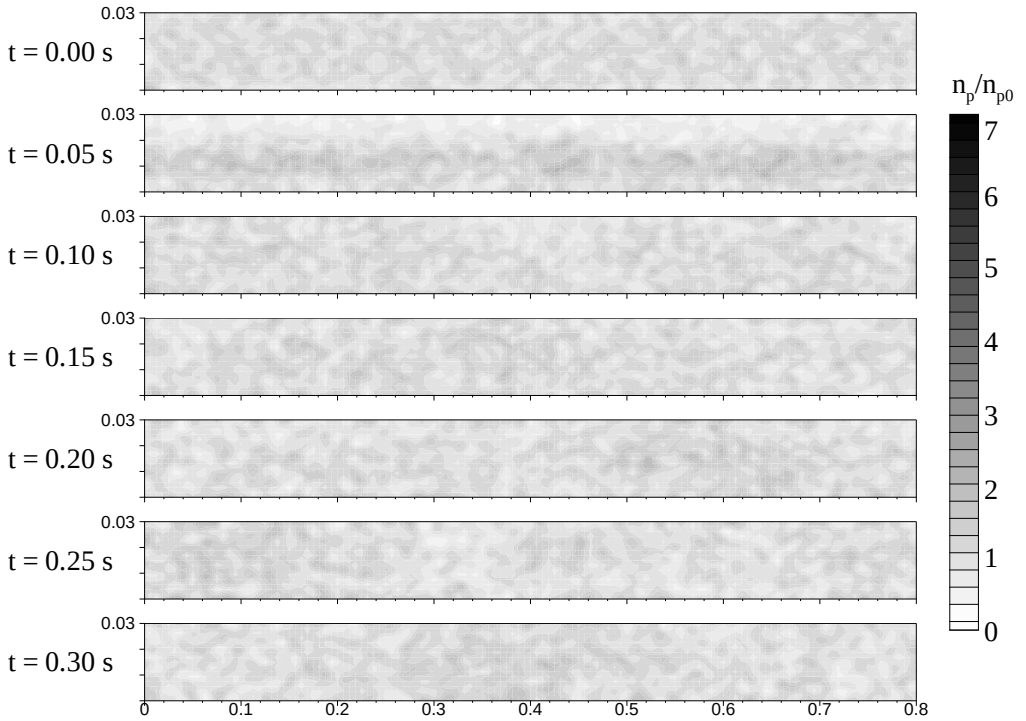

Figure 7: Distribution of relative number density over time for $\eta = 1$.

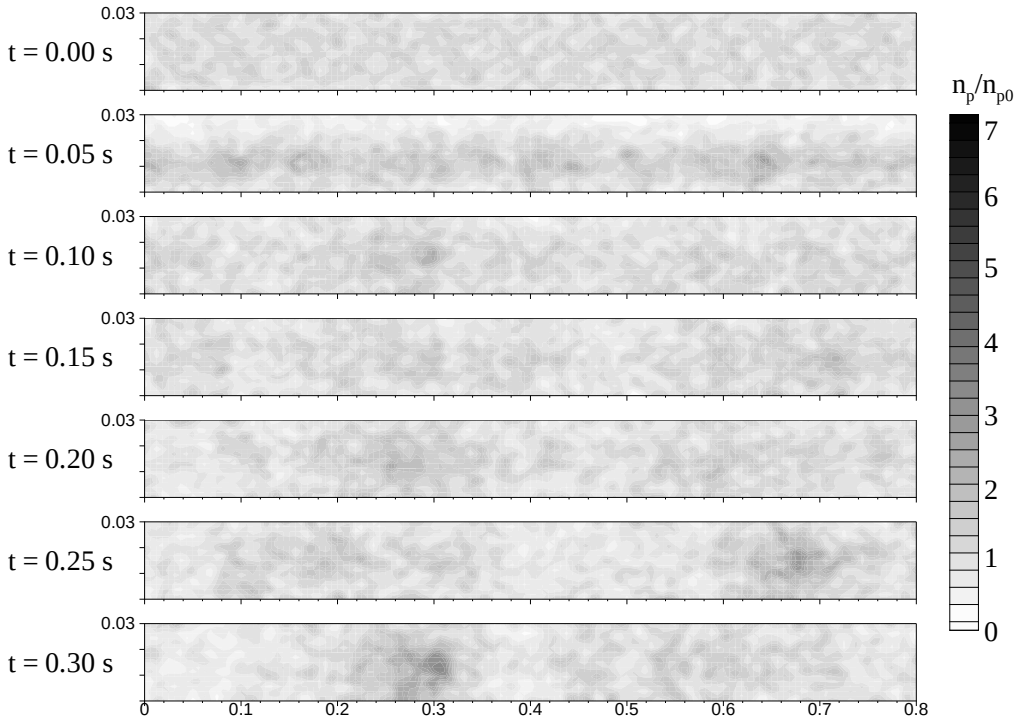

Figure 8: Distribution of relative number density over time for $\eta = 2$.

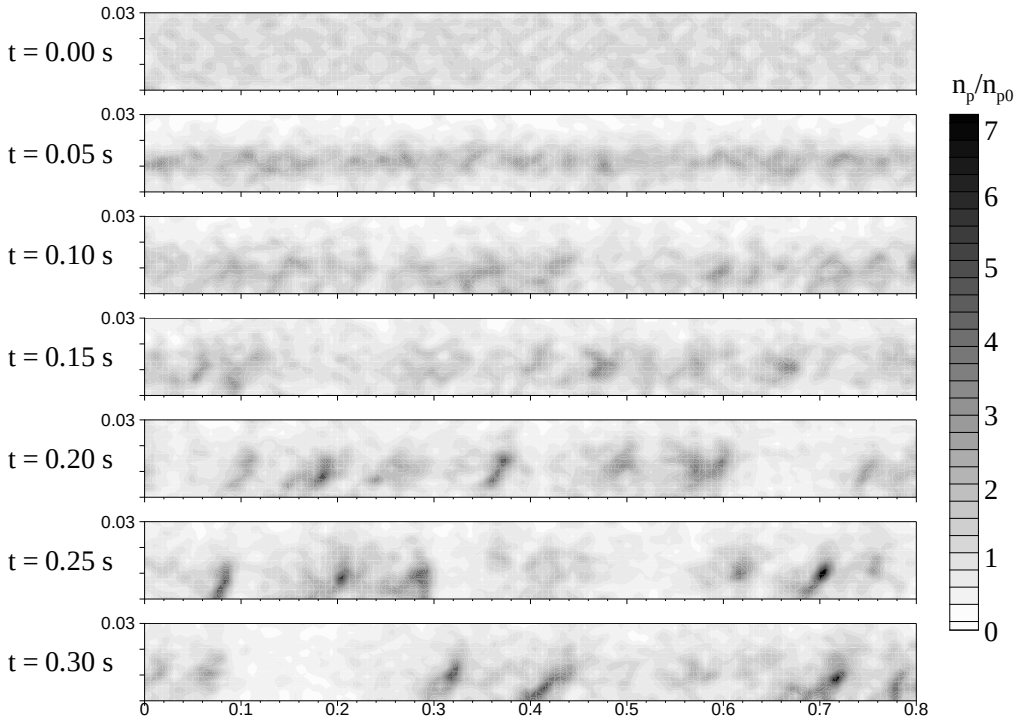

Figure 9: Distribution of relative number density over time for $\eta = 5$.

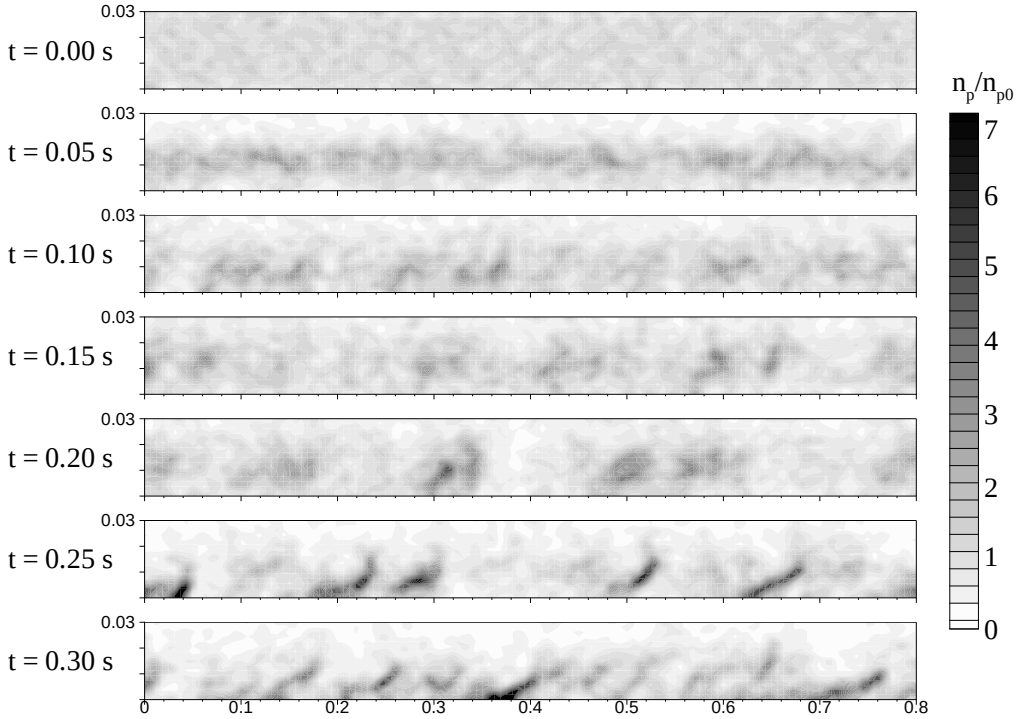

Figure 10: Distribution of relative number density over time for $\eta = 10$.

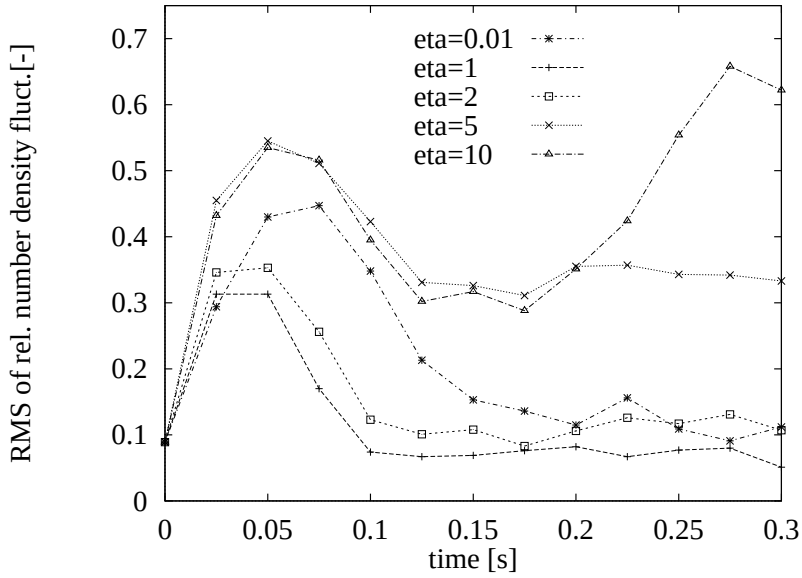

Figure 11: RMS of relative number density fluctuation $n_{fluct,RMS}$.

in the cases discussed before. Furthermore, the inhomogeneity does not vanish in the course of the simulation. The particle flow becomes even more and more inhomogeneous also in horizontal direction. Local areas of high concentration develop where the relative number density rises up to $n_P/n_{P0} \approx 7$. In the present paper these areas may be called "clusters", although in a non–compressed image they rather look like "garlands". Clusters seem to formate and grow around "cores", i.e. small local areas of higher number density induced by stochastic concentration fluctuations. Particles penetrating a cluster can be "captured" since the large number of collisions they undergo there cause their momentum to be adapted to that of the cluster particles. The center of most clusters is located between the channel axis and the bottom wall. This corresponds to the horizontally averaged data shown in figure 4. As one can see in figures 9 and 10 clusters do not constantly grow, but also thin and vanish. In the process of cluster breakup the interaction of cluster particles with the bottom wall seems to play an important role.

A quantitative measure of the inhomogeneity of concentration distribution is given by the root mean square of the fluctuation of relative number density $n_{fluct,RMS}$, which is computed as follows:

$$n_{fluct,RMS} = \sqrt{\overline{\left(\frac{n_P}{n_{P0}} - 1\right)^2}} \,. \tag{27}$$

In figure 11 $n_{fluct,RMS}$ is shown as it develops in time for all loading ratios considered in this paper. The value of $n_{fluct,RMS}$ at $t = 0\ s$ corresponds to the homogeneous concentration distribution obtained by randomly distributing the particles in the flow field. As already seen in figures 6–10 inhomogeneity increases at the beginning of the simulation for all loading ratios. For the dilute flow the maximum of $n_{fluct,RMS}$ is reached at about $t = 0.075\ s$. After that $n_{fluct,RMS}$ decreases down to the level of a homogeneous distribution, which is reached at about $t = 0.2\ s$. In contrast to the dilute case for $\eta = 1$ and $\eta = 2$ the maximum of $n_{fluct,RMS}$ is lower and also the flow becomes homogeneous much quicker. Obviously in these cases particle–particle collisions enhance dispersion. The collisions damp the development of inhomogeneities and enhance their dissolution. In the cases of $\eta = 5$ and $\eta = 10$ the initial increase in $n_{fluct,RMS}$ is stronger than in the other cases. Furthermore, after reaching its maximum at $t = 0.05\ s$ $n_{fluct,RMS}$ is only partly reduced. For $\eta = 5$ it remains almost constant on a higher level, whereas for $\eta = 10$ it even increases again for $t > 0.175\ s$. In these two cases inter–particle collisions enhance the development of an inhomogeneous concentration distribution and damp the dissolution of inhomogeneities.

5 Conclusion

Simulations of gas–solid flows in a horizontal channel were presented. The simulations were transient applying the Simulataneous Particle Tracking technique. Particle–Particle collisions were accounted for using a stochastic model. Simulations were carried out for different particle loadings in order to examine the influence of loading and collisions on the motion of the particle phase. The change of gas flow properties due to the presence of particles was not considered.

Particle–particle collisions were found to have a great effect on the particle concentration distribution in the channel. For particle to gas mass loading ratios of $\eta = 1$ and $\eta = 2$ collisions tended to enhance particle dispersion, whereas for higher loading ratios of $\eta = 5$ and $\eta = 10$ collisions enhanced the development of "clusters", i.e. local areas of higher particle concentration.

In the simulations presented in this paper mass loading was the only parameter that was varied. Of course there are many other physical and geometrical parameters that may influence the flow behaviour significantly, e.g. particle size and shape, gas velocity, channel size, phase coupling and so on. Hence there are many more simulations as well as experimental investigations necessary in order to understand the mechanisms of cluster formation and development.

Acknowledgements

The work presented in this paper was supported by the German Research Foundation (Deutsche Forschungsgemeinschaft – DFG) through the Collaborative Research Centre (Sonderforschungsbereich – SFB) 393. All simulations presented here were carried out on the Cray T3D at Edinburgh Parallel Computing Centre (EPCC) with support of the TRACS programme of the European Community.

References

Bird, G. A., 1976. *Molecular gas dynamics*, Oxford University Press.

Bird, G. A., 1989. Perception of numerical methods in rarefied gas dynamics. *Progr. Astro. and Aero.* **118**, pp. 211–226.

Bird, G. A., 1994. *Molecular gas dynamics and the direct simulation of gas flows*, Clarendon Press, Oxford.

Dennis, S.C.R., Singh, S.N. & Ingham, D.B., 1980. The steady flow due to a rotating sphere at low and moderate Reynolds numbers. *J. Fluid Mech.* **101**, pp. 257–279.

Illner, R., Neunzert, H., 1987. On simulation methods for the Boltzmann equation. *Transport Theory and Statistical Physics* **16**, pp. 141–154.

Kitron, A., Elperin & T., Tamir, A., 1989. Monte Carlo analysis of wall erosion and direct contact heat transfer by impinging two–phase jets. *J. Thermophysics* **3**, No. 2, pp. 112–122.

Kitron, A., Elperin & T., Tamir, A., 1990. Monte Carlo simulation of gas–solids suspension flows in impinging stream reactors. *Int. J. Multiphase Flow* **16**, No. 1, pp. 1–17.

Milojević, D., 1990. Lagrangian stochastic–deterministic (LSD) prediction of particle dispersion in turbulence. *Particle and Particle Systems Characterization* **7**, pp. 181–190.

Morsi, S.A. & Alexander, A.J., 1972. An investigation of particle trajectories in two–phase flow systems. *J. Fluid Mech.* **55**, No. 2, pp. 193–208.

Oesterlé, B. & Petitjean, A., 1991. Simulation of particle–to–particle interactions in gas–solid flows. *Proc. Int. Conf. on Multiphase Flows '91*, Tsukuba, Japan, Vol. 1, pp. 91–94.

Oesterlé, B. & Petitjean, A., 1993. Simulation of particle–to–particle interactions in gas–solid flows. *Int. J. Multiphase Flow* **19**, No. 1, 199–211.

Sommerfeld, M., 1992. Modelling of particle-wall collisions in confined gas–particle flows. *Int. J. Multiphase Flow* **18**, No. 6, pp. 905–926.

Tanaka, T., Kiribayashi & K., Tsuji, Y., 1991. Monte Carlo simulation of gas–solid flow in vertical pipe or channel. *Proc. Int. Conf. on Multiphase Flows '91*, Tsukuba, Japan, Vol. 2, pp. 439–442.

Tanaka, T. & Tsuji, Y., 1991. Numerical simulation of gas–solid two–phase flow in a vertical pipe: On the effect of inter–particle collision. *ASME FED–Vol. 121, Gas–Solid Flows*, Book No. G00609, pp. 123–128.

Tsuji, Y., Morikawa, Y. & Mizuno, O., 1981. Experimental measurement of the Magnus–force on a rotating sphere at low Reynolds numbers. *Transactions of ASME, J. Fluids Eng.* **107**, pp. 484–488.

Yonemura, S., Tanaka & T., Tsuji, Y., 1993. Cluster formation in gas–solid flow predicted by the DSMC method. *ASME FED–Vol. 166, Gas–Solid Flows*, Book No.H00806, pp. 303–309.